

## Intensification of Plasma Upflows in an Active Region—Coronal Hole Complex: A CME Precursor

D. Baker,<sup>1</sup> L. van Driel-Gesztelyi,<sup>1,2,3</sup> M.J. Murray,<sup>1</sup> L.M. Green,<sup>1</sup>  
T. Török,<sup>2</sup> and J. Sun<sup>1</sup>

<sup>1</sup>*University College London, Mullard Space Science Laboratory,  
Holmbury St. Mary, Dorking, Surrey, RH5 6NT, U.K.*

<sup>2</sup>*LESIA, Observatoire de Paris, CNRS, UPMC, Université Paris  
Diderot, 5 place Jules Janssen, 92190 Meudon, France*

<sup>3</sup>*Konkoly Observatory of Hungarian Academy of Sciences, Budapest,  
Hungary.*

**Abstract.** We investigate the plasma flows resulting from the interaction between a mature active region (AR) and a surrounding equatorial coronal hole (CH) observed by *Hinode*'s EIS and XRT from 15 to 18 October 2007. For 3 days, EIS velocity maps showed upflows at the AR's eastern and western edges that were consistently between 5 and 10 km s<sup>-1</sup>, whereas downflows of up to 30 km s<sup>-1</sup> were seen in AR loops. However, on 18 October, velocity profiles of hotter coronal lines revealed intensification in upflow velocities of up to 18 km s<sup>-1</sup> at the AR's western footpoints 4.5 hours prior to a CME. We compare the AR's plasma flows with 2.5D MHD numerical simulations of the magnetic configuration, which show that expansion of the mature AR's loops drives upflows along the neighboring CH field. Further, the intensification of upflows observed on the AR's western side prior to a CME is interpreted to be the result of the expansion of a flux rope containing a filament further compressing the neighboring CH field.

### 1. Observations

Multi-wavelength data were used to follow the evolution of a mature AR embedded in an equatorial CH from 15 to 18 October 2007. Data from *Hinode*'s EUV Imaging Spectrometer (EIS) provided the means by which we were able to examine multi-temperature plasma flows in the AR. Standard SolarSoft routines were used to calibrate and process all data. Instrumental effects including orbital variation and slit tilt were removed.

Fig. 1 shows *Hinode*'s X-Ray Telescope (XRT) full disk (left) and zoomed (right) images of the AR and surrounding CH on 17 October. The small AR was measured to have magnetic flux of  $3 \times 10^{21}$  Mx. Overall, the magnetic configuration of the AR appears highly sheared throughout the observation period (see Fig. 1, right panel). A filament, lying along the internal polarity inversion line and co-spatial with the bright sigmoidal loops towards the (solar) northwestern side of the AR, is evident in both H $\alpha$  and *TRACE* 171 Å data on the 17<sup>th</sup> and 18<sup>th</sup> (not shown). At approximately 07:35 UT on the 18<sup>th</sup>, the southwestern section of the AR erupts and a few hours later, a small CME is visible in LASCO's C2 Coronagraph data.

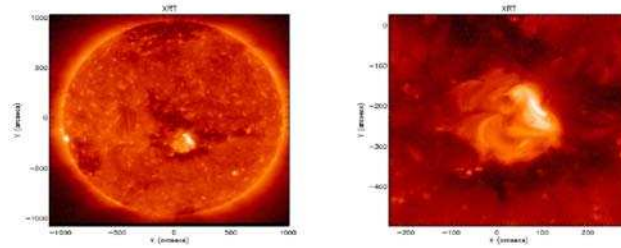


Figure 1. *Hinode* XRT thin al mesh filter full disk (left) and zoomed (right) images of the mature AR inside an equatorial CH. The AR’s sigmoidal magnetic structure is evident in the image on the right.

## 2. Active Region Plasma Flows

EIS 195 Å velocity maps created from EIS rasters obtained between 15 and 18 October show that there are a series of loop structures connecting positive to negative magnetic field concentrations at the AR’s footpoints (Fig. 2a and 2b). These loops are clearly red-shifted, indicating downflows within the loops. Downflows are persistent throughout the observation period. Line of sight downflow velocities range from a few  $\text{km s}^{-1}$  to  $35 \text{ km s}^{-1}$ .

Blue-shifted upflow regions are observed at the periphery of the AR on both the east and west. Though the location of the upflows changes slightly from day to day, the upflows continue to originate at the periphery of the AR over areas of positive and negative field concentrations (Fig. 2a). Upflow velocities range from approximately  $5$  to  $10 \text{ km s}^{-1}$  from 15 to 17 October. Upflows on both sides of the AR occur in hotter coronal emission lines e.g. Fe X ( $T = 1 \text{ MK}$ ), Fe XI ( $T = 1.3 \text{ MK}$ ) and Fe XIII ( $T = 1.6 \text{ MK}$ ) but are less pronounced in cooler lines such as Fe VIII and Si VII ( $T = 600,000 \text{ K}$ ). At 00:18 UT on 18 October, velocity profiles reveal a distinct intensification of upflow velocities in the western upflow region to  $18 \text{ km s}^{-1}$ . Fig. 2c shows velocity profiles along  $Y = -190''$  and  $Y = -225''$  in the velocity map from the 18<sup>th</sup>. We see similar intensification in upflow velocities on the 18<sup>th</sup> in all reasonably unblended coronal lines.

## 3. Simulations

We carried out 2.5D simulations (see Murray et al. 2009) of flux emerging in a CH to investigate where flows arise and what is driving them. The simulations show three types of flows. Two types of flows are a direct consequence of reconnection between the AR and CH fields producing: (1) hot, fast jets on the reconnecting (east) side of the AR, and (2) slow, cool plasma upflows driven by an enhanced gas pressure gradient acting along newly opened field on the west. These plasma flows, usually associated with new flux emergence, have properties significantly different to the plasma properties we observed in the mature active region.

A third type of plasma flows is driven by AR loop expansion which compresses or ‘squeezes’ the plasma tied to the neighboring open CH field. Fig.

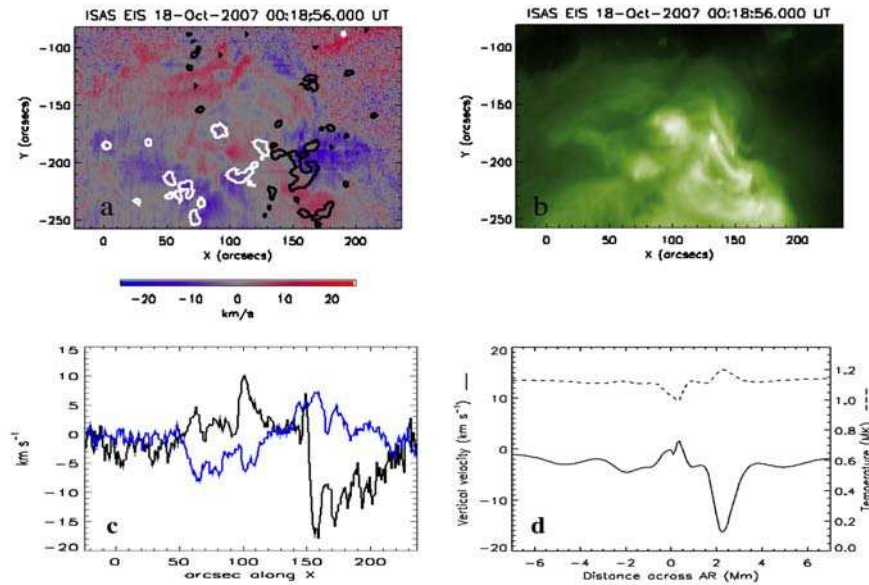


Figure 2. a: *Hinode* EIS 195 Å velocity map overlaid with *SOHO* MDI 100 G contours (black = negative and white = positive polarities). Blue-shifted upflows occur over areas of concentrated magnetic field. b: *Hinode* EIS 195 Å intensity map for 18 October 2007 00:18 UT. c: Velocity profiles along  $Y = -225''$  (blue) showing maximum velocity in the eastern upflow region and  $Y = -190''$  (black) showing intensification of upflows in the west. d: From 2.5D simulations, vertical velocity (solid line) and temperature (dashed line) along a cut across the AR showing properties consistent with EIS observations.

2d shows vertical velocity and temperature measured across the AR where we see the blue-shifted upflows in the EIS velocity maps. Properties of the upflows include: location = over western footpoints; upflow velocity range = 0-20 km s<sup>-1</sup>; upflow temperature = 0.15-1.2 MK. These properties are consistent with upflows observed by EIS.

#### 4. Discussion

The simulations show that where surrounding field is not aligned for reconnection with the AR, slow upflows occur at the periphery of the AR as a result of the expansion of the closed AR loops. This is consistent with *Yohkoh* SXT observations carried out by Uchida et al. (1992) who found almost continuous expansion of loops in ‘active’ ARs. We observed persistent upflows which we interpret to be the result of the continuous, slow expansion of the AR driving upflows along surrounding magnetic field at the AR’s periphery. Expansion in a mature AR may be due to magnetic diffusion and/or cancellation along the magnetic inversion line increasing the AR’s non-potentiality.

Intensification of upflow velocities observed on the western side of the AR requires greater compressive forces there. A flux rope containing a filament located closer to the western side of the AR is a possible source of additional compressive forces. Between 17:00 to 18:30 UT on the 17<sup>th</sup>, the AR expands

and there is a small eruption to the northeast. The AR goes through a failed eruption close to its core at 04:30 UT and finally erupts at 07:35 UT towards the southwest, leading to the CME seen in LASCO's C2. Pre-eruption expansion of the flux rope containing the filament could provide the required increase in compressive forces causing intensification of upflows from less than  $10 \text{ km s}^{-1}$  to  $18 \text{ km s}^{-1}$  seen at 00:18 UT on the 18<sup>th</sup>.

Examination of time sequences of MDI magnetograms shows that opposite polarity flux converges and cancels in the vicinity of the filament hours before the northeastern expansion and again, early on the 18<sup>th</sup>, prior to the failed and main eruptions. Location of the flux cancellation on the 18<sup>th</sup> is spatially coincident with the center of the transient sigmoid which forms during the eruption. Measurements of the flux values from MDI magnetograms show that flux falls by  $\approx 10^{21}$  Mx (or 10% of total flux per day) throughout the expansion of the AR and series of eruptions, which we suggest destabilizes the tied-down field by flux cancellation (tether cutting; Moore et al. 2001) thus increasing twist in the flux rope and yielding slow expansion and eventual eruption of the flux rope.

## 5. Summary

We propose a mechanism to explain in this particular magnetic configuration the origin of persistent enigmatic upflows seen at the AR's periphery. Simulation results show that a plausible mechanism for such upflows is AR loop expansion which drives upflows along neighboring "open" CH field. This mechanism can explain ubiquitous upflows observed along the periphery of ARs if there is open field in the surrounding field. Substantial flux cancellation (10% of total AR flux per day) leading up to the CME eruption is suggestive of the tether cutting mechanism being involved in the CME initiation. Intensification of upflows prior to eruptive activity in the AR-CH complex can be recognized as a pre-CME signature.

**Acknowledgments.** DB and MJM acknowledge financial assistance from the Science and Technology Facilities Council (STFC). LvDG acknowledges the Hungarian government grant OTKA 048961. The computational work for this paper was carried out in the joint STFC and SFC (SRIF) funded linux cluster at the University of St Andrews (Scotland, UK). *Hinode* is a Japanese mission developed and launched by ISAS/JAXA, with NAOJ as domestic partner and NASA and STFC (UK) as international partners. It is operated by these agencies in co-operation with ESA and the NSC (Norway). The authors thank MDI and LASCO teams for their data. *SOHO* is a project of international cooperation between ESA and NASA.

## References

- Moore, R. L., Sterling, A. C., Hudson, H. S., and Lemen, J. R., 2001, ApJ, 552, 833.  
 Murray, M. J., van Driel-Gesztelyi, L., and Baker, D., 2009, A&A (submitted).  
 Uchida, Y., McAllister, A. Strong, K. T., Ogawara, Y., Shimizu, T., Matsumoto, R. and Hudson, H. S., 1992, PASJ, 44, L155.